RRS James Cook JC102

Cruise Report

The Role and Extent of Detachment Faulting at Slow-Spreading Mid-Ocean Ridges

Leg 1

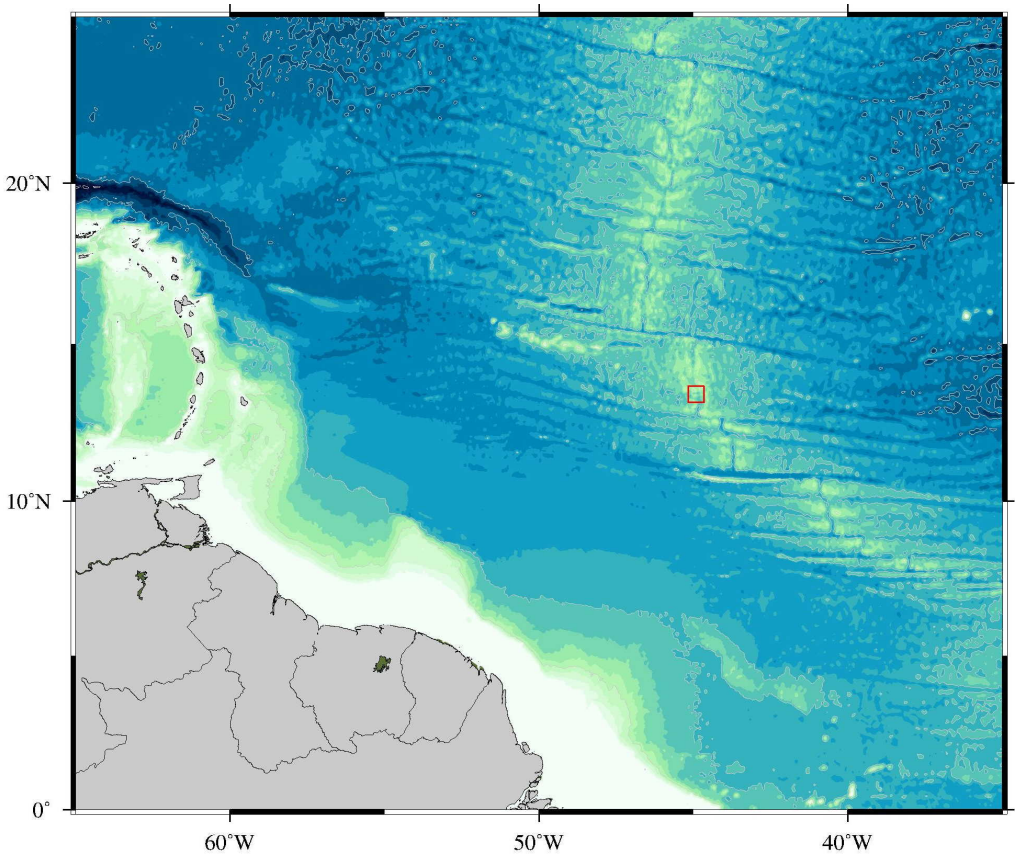

6th– 18th April 2014

Port of Spain (Trinidad) – Port of Spain (Trinidad)

RRS James Cook JC102

Cruise Report

The Role and Extent of Detachment Faulting at Slow-Spreading Mid-Ocean Ridges

Leg 1

6th – 18th April 2014
Port of Spain, Trinidad – Port of Spain, Trinidad

Prof Christine Peirce

Department of Earth Sciences
University of Durham
South Road
Durham
DH1 3LE

christine.peirce@durham.ac.uk

April 2014

Table of Contents

Courtesy of Andrew Clegg

Summary

The primary objective of RRS James Cook cruise JC102 was to install 25 ocean-bottom seismographs at the 13° 20´N oceanic core complex on the Mid-Atlantic Ridge, to record local passive micro-seismicity. These instruments will be recovered during JC109, six months after deployment. Gravity and swath bathymetry data were also acquired port-to-port, with the gravity data tied against two relative stations established on the quayside, and the swath bathymetry data calibrated with a sound velocity dip undertaken at the lateral centre of the ocean-bottom seismograph grid.

1. Background and scientific objectives

1.1 Background

Since the discovery of domal corrugated surfaces at slow-spreading mid-ocean ridges (Cann et al., 1997), our understanding of how seafloor spreading works has radically changed. These domal surfaces, termed oceanic core complexes, were believed to be the unroofed plutonic and partially serpentinized mantle footwalls of large-offset normal 'detachment' faults; structures apparently responsible for accommodating much of the plate separation. These detachment faults are believed to cross-cut the entire crust, exhuming in their footwalls first a crustal section (typically a non-corrugated blocky massif) and then, in the domal oceanic core complex (OCC - Fig. 1), mantle rocks intruded by plutonic gabbros (Tucholke and Lin, 1994; Cann et al., 1997; Tucholke et al., 1998). The OCC is commonly striated and corrugated in the spreading direction (Fig. 1) and interpreted to be a slip surface, exhumed from beneath median valley basalts.

Many aspects of this newly recognised mode of seafloor spreading remain unproven or controversial. For example, although it is likely that the corrugated upper surfaces of OCCs represent the exposure of steeply dipping detachments rooting at depth beneath the median valley, the link has not been clearly proven, though it is supported to some extent by palaeomagnetic studies (Morris et al., 2009; MacLeod et al., 2011) that show significant footwall rotation.

The only in situ evidence to date is based on P-wave travel-time tomographic inversion of two 2D wide-angle seismic profiles and passive micro-seismicity monitoring near the TAG hydrothermal field (Fig. 2 - deMartin et al., 2007). There, a steeply dipping band of hypocentres is inferred to mark a fault that flattens abruptly upwards to follow an unconnected, shallower, gently-dipping boundary between two velocity anomalies, one of which, reflecting a region of higher relative velocity, is located in the footwall.

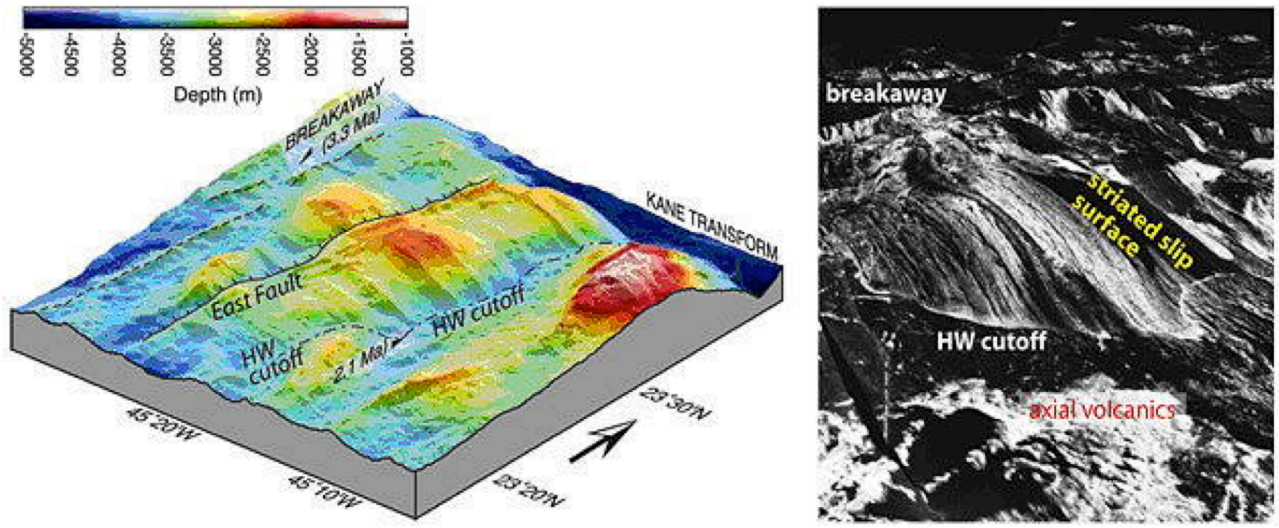

Figure 1: Perspective views of two typical Atlantic OCCs: Kane B (left) and 1320 (right). Both show corrugated/striated exhumed slip surfaces, the breakaway and hanging-wall cut-offs, but whereas Kane B has been rafted off-axis and so is no longer actively being exhumed, 1320 is still being pulled out from beneath a gap (dark area bottom right) in a zone of axial volcanics (rough, light tones).

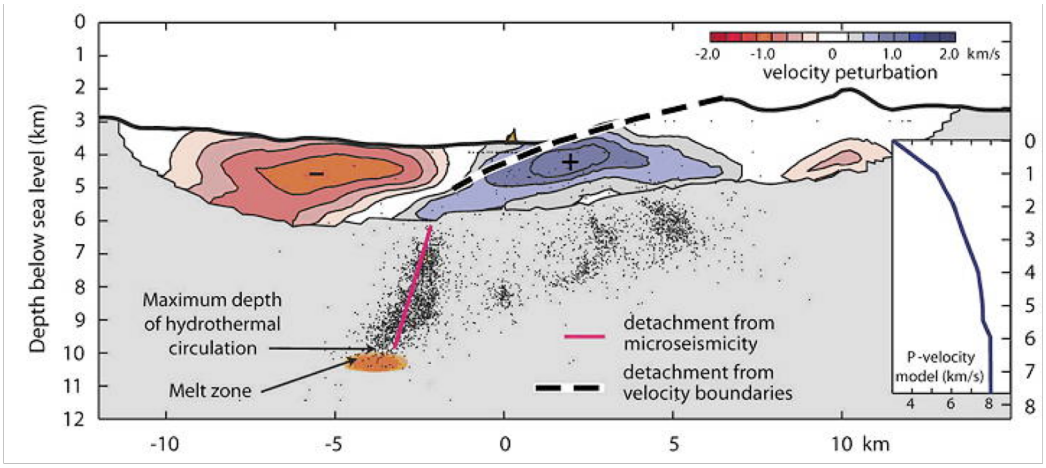

Figure 2: Section through the TAG area (deMartin et al., 2007), showing a possible detachment partly defined as a velocity boundary and partly as a zone of dipping micro-seismicity.

However, the TAG data does not directly image the detachment rollover, does not prove the continuity between steep and shallow zones, and does not show the lateral extent of the detachment.

Escartín et al. (2008) and Reston & Ranero (2011) see oceanic detachment faults as essentially continuous, long-lasting features active on a segment scale (Fig. 3). Here, OCCs are simply places where a mega-detachment breaks surface, being covered in the intervening regions by thin-skinned rider blocks of volcanic seafloor. If so, as much as 50% of Mid-Atlantic Ridge (MAR) crust may be the result of asymmetric detachment faulting; it has even been suggested that mantle-derived material may dominate huge swathes of Atlantic ocean floor, potentially forming 20-25% of all seafloor produced at spreading rates <40mm/yr (Cannat et al., 2010).

Alternatively, MacLeod et al. (2009) see OCCs as spatially restricted, ephemeral features that are switched on and off by variations in local magma supply (Fig. 4). In this model OCC detachments are ordinary valley wall faults on which slip continues as a result of the progressive waning of magma supply to below half that needed to generate a continuous igneous crustal layer. Strain localisation would result in progressively more asymmetric plate separation, until more than half is partitioned onto the detachment itself. As this occurs, the detachment migrates towards and across the axial valley, such that renewed magmatism is intruded into the detachment footwall and ultimately overwhelms it. Spreading becomes strongly asymmetric between a localised OCC and its immediate conjugate, but not across the whole of a spreading segment. The lateral change in spreading asymmetry and the limited dimensions of the detachment fault in this model require spatially restricted transfer zones (dominated by magmatism and ductile shear at depth and faulting near surface) to accommodate the along-strike variations in strain distribution.

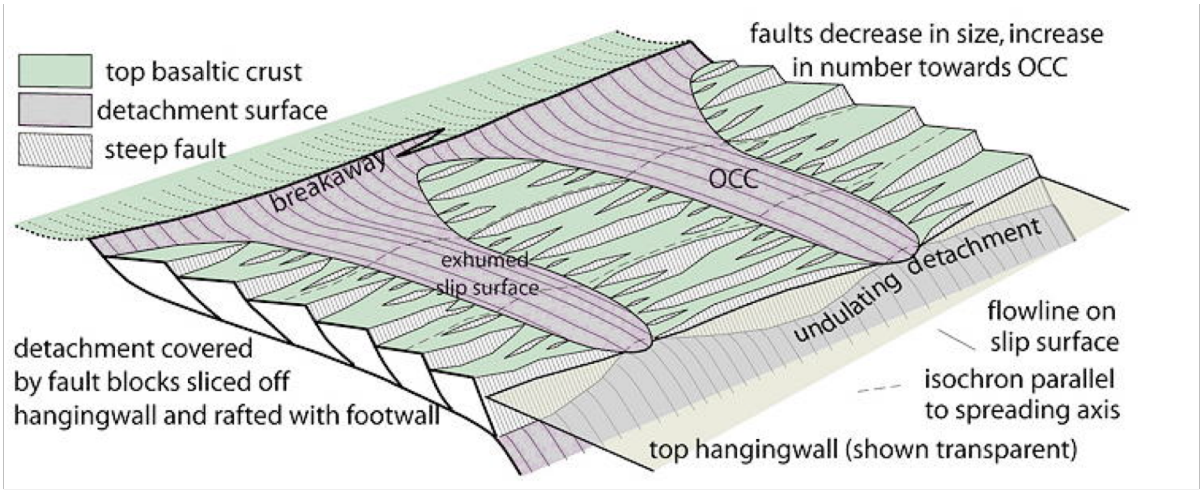

Figure 3: Perspective view of the segment scale detachment model: the detachment continues laterally beneath small fault blocks between adjacent OCCs, which represent the places where the detachment breaks the surface. In the alternative model, adjacent OCCs are unconnected.

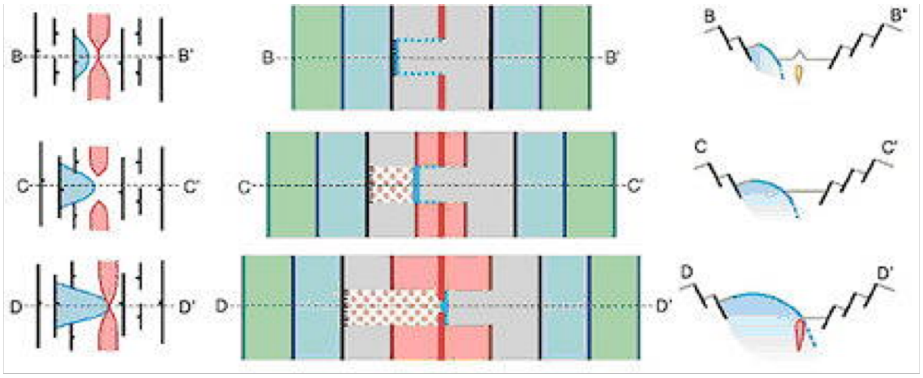

Figure 4: MacLeod et al. (2009) model for OCC formation: strain weakening concentrates deformation onto a single fault which accommodates more than half the total spreading, and so migrates toward and over the spreading axis, to be cut by renewed magmatism. Left: structural map; Middle: magnetic lineations; Right: schematic sections.

There are, therefore, two conflicting hypotheses:

1) detachments continue laterally between OCCs which are linked (Reston and Ranero, 2011)

and

2) detachments are temporally and spatially restricted and not linked (MacLeod et al., 2009).

The two conflicting hypotheses (**1. linked vs. 2. restricted**) make testable predictions:

1a: Detachments continue in the sub-surface between OCCs and so control divergence at a whole spreading segment for extensive periods of time;
1b: Asymmetric spreading affects the whole segment, not just OCCs and their conjugates;
1c: By controlling spreading of an entire segment, the detachment drives mantle upwelling and location of the spreading axis.

2a: Detachments are restricted to individual OCCs and are thus localised in time and space;
2b: OCCs produce spatially restricted spreading asymmetry that does not extend segment-wide; strain is transferred laterally by magma injection and brittle deformation;
2c: Gabbros are only incorporated into the footwall late as it migrates across the median valley.

We can test the above hypotheses by determining:

(a) the sub-surface geometry of detachment faults at active OCCs, and how this changes in extent both along- and across-strike beneath adjoining volcanic-dominated seafloor;
(b) the local degree of asymmetry of plate separation adjacent to an OCC compared to the adjoining volcanic seafloor; and
(c) the amount and distribution of melt delivered to both hanging wall and footwall at an active OCC in comparison to that in the adjoining volcanic seafloor region.

The required data from an actively forming OCC do not exist, and we will collect them during three cruises to the MAR between ~13°15' and 13°35'N. This report describes the first of these cruises – the passive micro-seismicity ocean-bottom seismograph deployment.

1.2 The study location - 13°N

An extensive region of OCCs exists at 13°N on the MAR, and includes two located at 13°20'N (henceforth known as 1320) and 13°30'N (1330) that are actively developing, making this region the ideal target for this study. These OCCs have already been surveyed with shipboard multi-beam swath bathymetry (Smith et al., 2008), imaged with TOBI near-bottom side-scan and sampled with dredges and a seabed rock-drill (Searle et al., 2007; MacLeod et al., 2009; Mallows, 2011; Mallows and Searle, 2012).

Apart from the wealth of existing data, 13°N is the ideal location for this study because:

- unlike other fully-developed OCCs both 1320 and 1330 can be traced directly to the spreading axis, implying that both are currently active;
- the typical, high reflectivity, untectonised hummocky terrain of the MAR neovolcanic zone (NVZ) is absent opposite 1320 and 1330 (Fig. 1), and is replaced by lower reflectivity terrain (suggesting older volcanics with several metres of sediment cover), often displaying small-scale faulting. This, and a concomitant increase in tectonic strain, is interpreted as evidence that the melt supply is reduced near the regions of active detachment faulting (MacLeod et al., 2009);
- the NVZs north and south of 1320 taper toward it, suggesting they are propagating towards this magmatic gap and may ultimately "switch off" the detachment faulting, as appears to have been the case for the off-axis OCC at 13°48'N; and finally and crucially
- the presence of two active OCCs that developed at similar times and which remain active implies either that the controlling detachment continues under the intervening basin or that the basin is a zone of magmatic soft linkage between two spatially limited detachment systems.

1.3 Scientific objectives

The primary objectives of this project are to test the different and contrasting hypotheses for the spatial and temporal evolution of OCCs. From all three cruises acquiring the necessary geophysical data, we will determine:

1) the geometry of the detachments that have unroofed the 1320 and 1330 OCCs, (i) through direct imaging of the detachment surface with multichannel seismic (MCS) reflection data, and (ii) by imaging with ocean-bottom seismograph (OBS) wide-angle (WA) data any intra-crustal layering (refracting interfaces) and regions of mantle-derived material and melt accumulation (relative velocity anomalies), in both cases from the seabed down to sub-Moho, and (iii) from the distribution of seismicity down to the base of the brittle lithosphere, probably 7-8 km sub-seafloor (testing **Hypotheses 1a, 1c, 2a, 2c**);
2) the lateral extent of the 1320 and 1330 detachments, through a combination of direct (MCS reflection) and indirect (WA velocity structure) imaging, and distribution of seismicity (testing **Hypotheses 1a, 2a**);
3) the detailed spreading history and thus any along-segment variation in the asymmetry of spreading, through high-resolution Autosub magnetic imaging (testing **Hypotheses 1b, 2b**);
4) the detailed internal structure of the footwall of the detachment, both at the spreading axis and at an OCC, through a combined approach of 3D seismic velocity tomography and magnetic field inversion (testing **Hypothesis 1c, 2c**); and
5) we will also collect high-resolution bathymetry data simultaneously with magnetic field measurements on Autosub 6000, which will aid structural interpretation of, for example, OCC domes, the inferred exhumed Moho and tectonic linkages. We will also use Autosub to identify locations of fluid outflow (fault scarps, hydrothermal systems and exposures on the corrugated surface – Connelly et al., 2011) and future sampling sites from the nephelometer, CTD, Eh and ADCP data collected contemporaneously with the high resolution bathymetry and magnetic data. These data will also constrain the precise geometry and extent of the hydrothermal discharge inferred at the toe of 1320 from the massive sulphides recovered there on JC007 (Searle et al., 2007), and thus inform our understanding of the thermal structure of the OCC and likely implications for controls on the larger-scale rheology.

Leg 1, JC102, aimed to deploy the OBS for a 6-month duration local micro-seismicity survey. Leg 2, JC109, aims to recover the OBS. Finally, Leg 3 aims to complete active-source MCS and WA seismic acquisition and Autosub 6000 surveying.

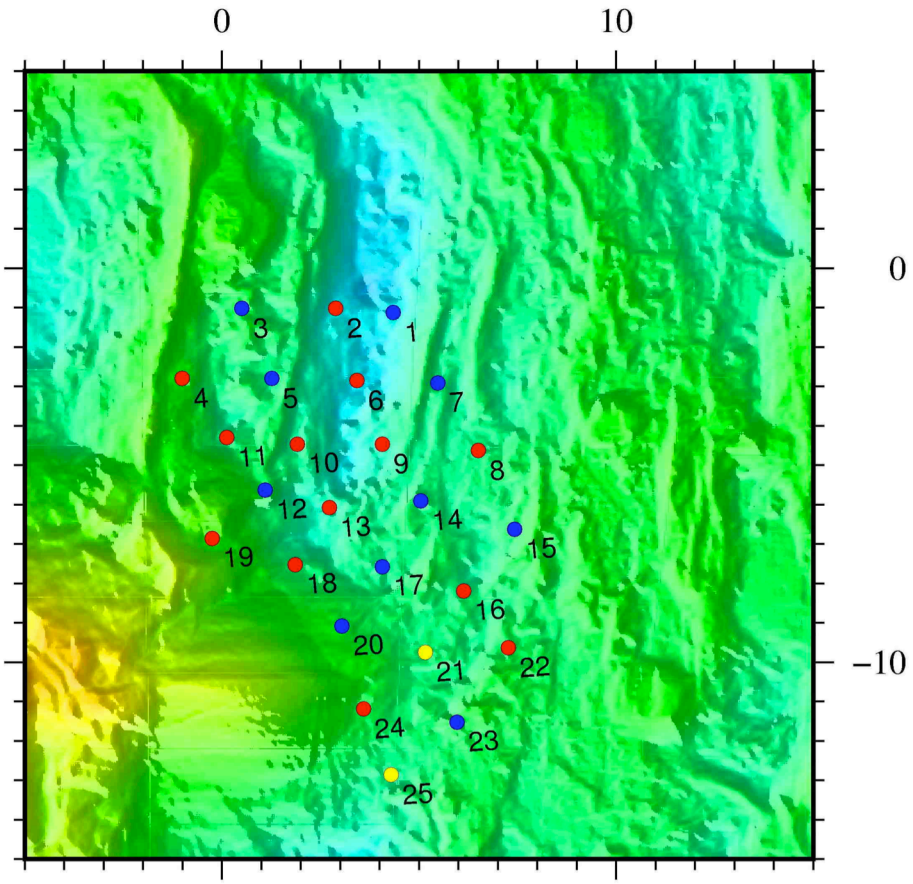

Figure 5: Planned OBS deployment locations for passive micro-seismicity recording. All OBS were equipped with a three-component 4.5 Hz, gimballed geophone pack. The red OBS were equipped with an hydrophone and the blue and yellow OBS with differential pressure gauges. The yellow OBS denote the use of entirely glass sphere flotation, while all other OBS were deployed with glass flotation supplemented with syntactic foam. Axes are in kilometres.

For JC102 we followed the approach adopted by project partner Sohn at the TAG area (deMartin et al. 2007). We planned to deploy 25 OBS in a tight network centred on the most ridgeward limit of the 1320 OCC and extending to the north (Fig. 5 for planned OBS locations). The deployment locations were planned to be concentrated over the northern half of the 1320 detachment, close to its hanging wall cut-off (where the detachment passes beneath the seafloor) and continue to the north approximately halfway towards the 1330 OCC, to map out the postulated lateral continuation of the master detachment between OCCs. Given the known amount of teleseismic activity from the study area, we estimate that ~50 locatable earthquakes will take place every day. By recording for 6 months, we expect to record ~9000 earthquakes and expect these to be representative of the active faulting in the region.

2. Cruise preparation and mobilisation

2.1 Scientific plan

The port call at the start of the cruise was Port of Spain (Trinidad), which was ~4 days from the work area at a transit speed of 10 kn. The entire science programme would take 4 days – 1.5 days of OBS deployment, sound velocity profile and acoustic release tests, followed by 2.5 days of swath bathymetry surveying. The end of cruise port call was also Port of Spain (Trinidad). The entire cruise was, thus, 12 days port-to-port. The way points for the cruise can be found in Table 1.

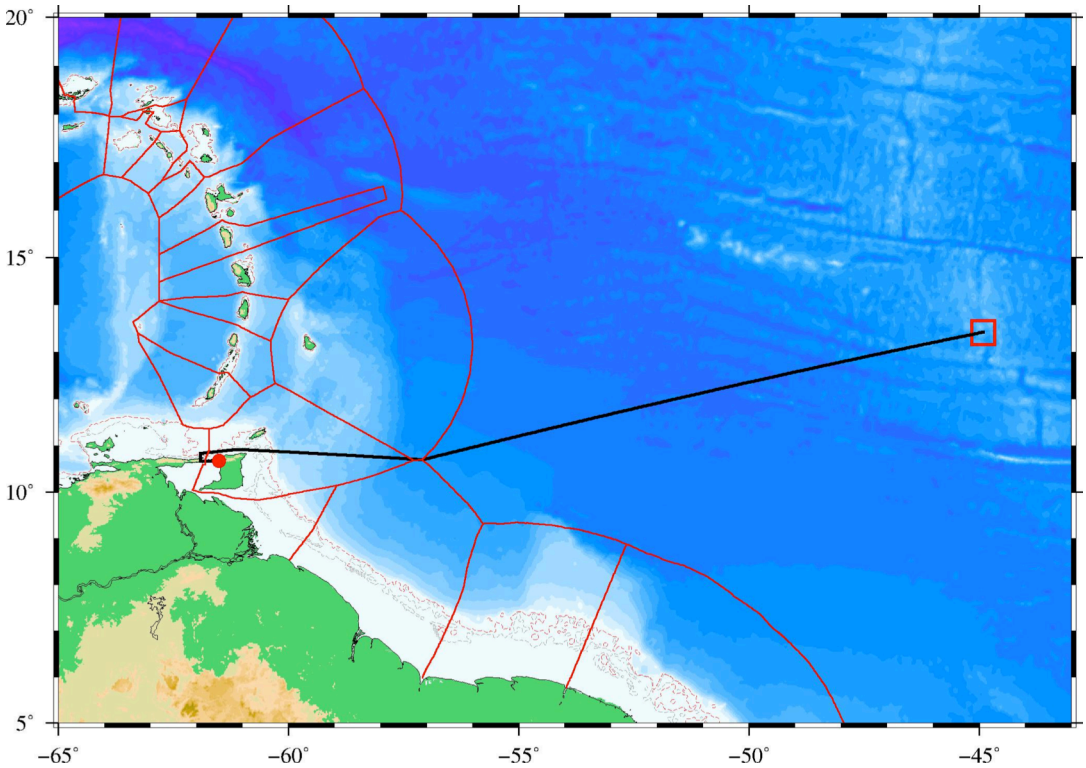

Figure 6: Work area plotted relative to the EEZ of the Caribbean region, together with the proposed transit track.

2.2 Territorial waters and diplomatic clearances

The work area for this cruise lies entirely in international waters as shown in Fig. 6. We also planned to run the gravimeter and swath bathymetry acquisition all the way from and to the ports of call to enable a start and end of cruise base station tie.

Consequently, diplomatic clearance from Trinidad and Tobago was required. This application was made in September 2013 and approval received just prior to departure.

2.3 Mobilisation

All equipment containers shipped from the UK were made available by the ship's appointed agent for unloading on arrival at the vessel. Mobilisation commenced on the 5th April with a sailing date of the 09:00 (local = GMT-4) 6th April. The port call activities solely related to the unloading and secure stowage of the OBSs and undertaking the gravity base tie, by establishing two relative base stations on the quay adjacent to the vessel.

Mobilisation went without any significant problems except for a mandatory piece of Bridge communications equipment that failed just prior to sailing. However, a fix was achieved with the assistance of a local engineer and the Cook sailed at 22:30 (local – 02:30 GMT 7th April) on the 6th April; a delay of 11:30hrs.

3. Work conducted and data collected

A track chart for the entire cruise is shown in Fig. 7, a blow-up of the work area only is shown in Fig. 8. The data acquisition comprised: i) ocean-bottom seismograph deployments; ii) sound velocity profiling; iii) gravity; and iv) swath bathymetry surveying. Each of these data types and the equipment used will be described in the following sections.

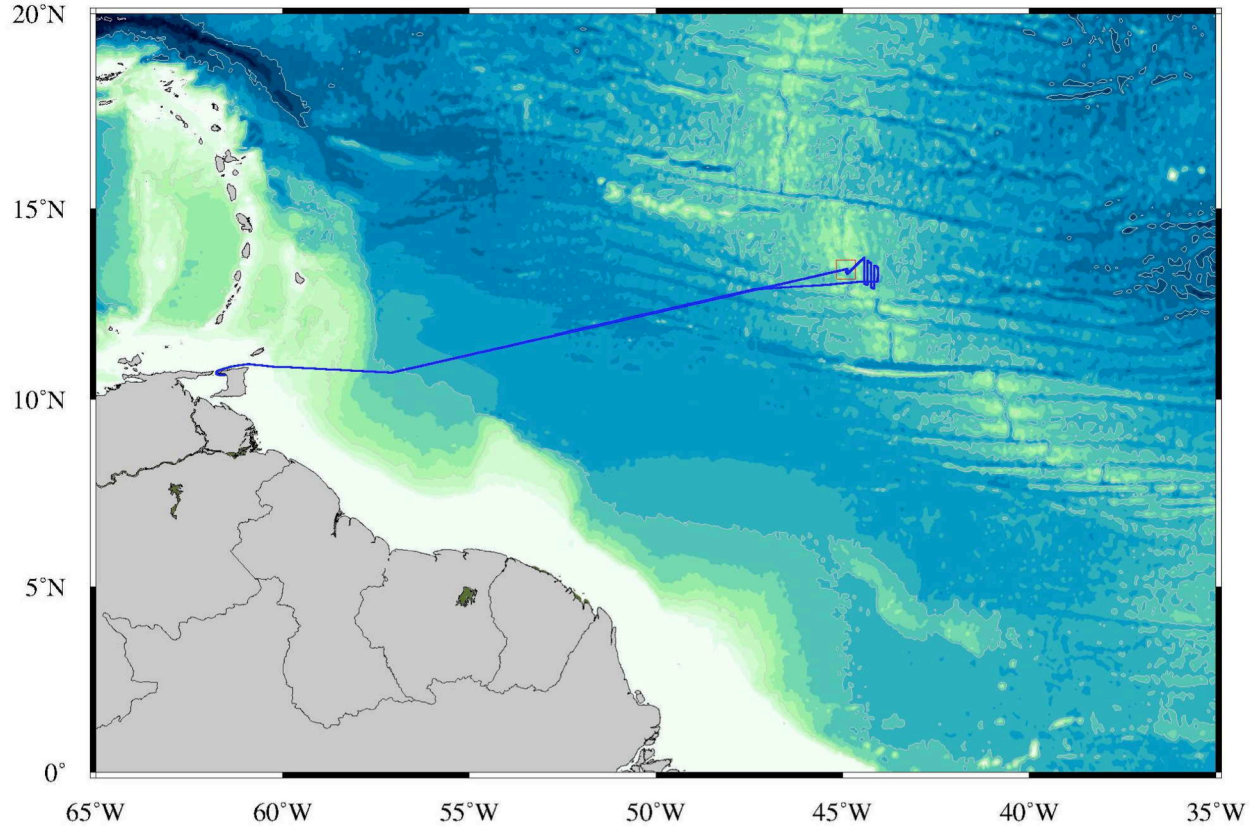

Figure 7: Track chart for JC102.

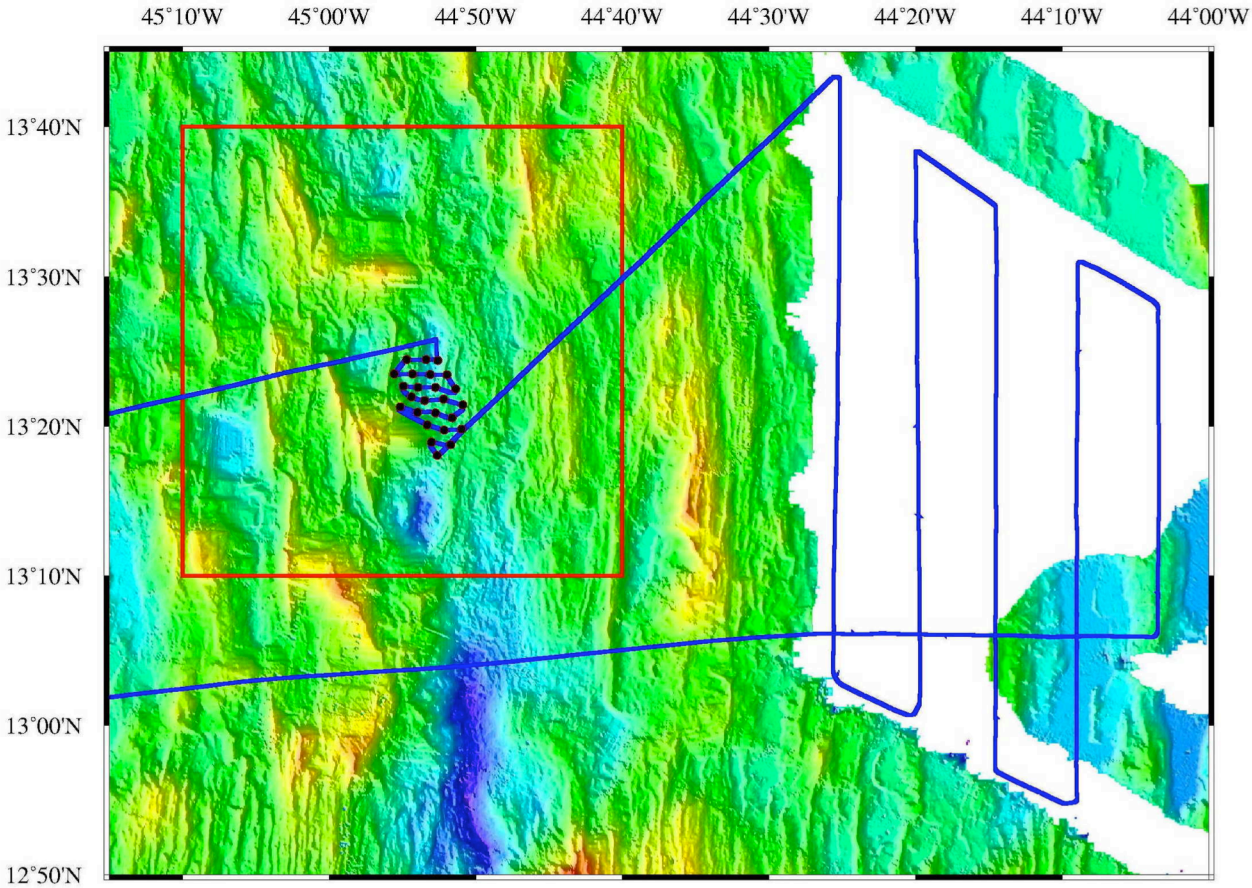

Figure 8: Track chart for the work area of JC102.

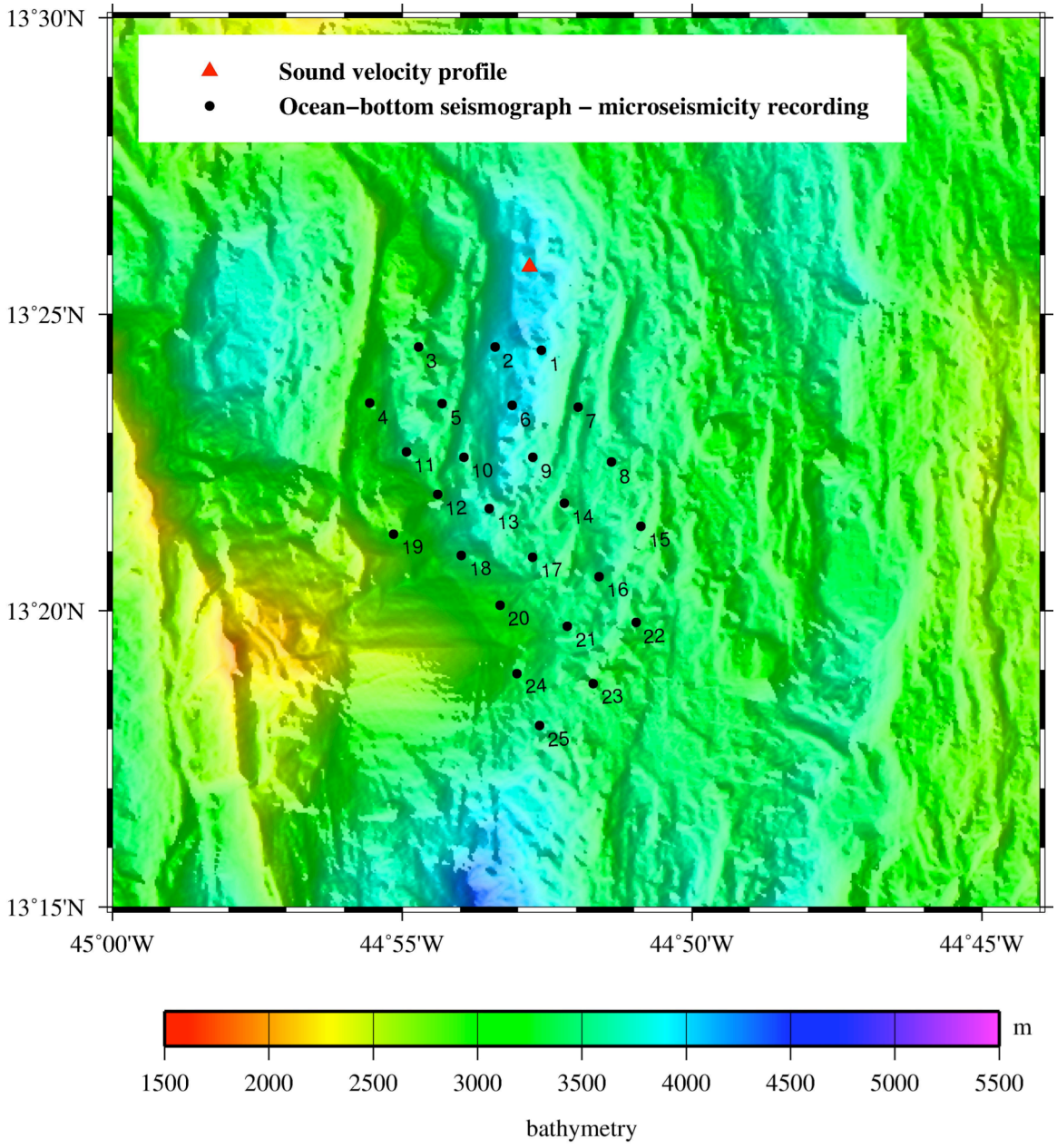

Figure 9: OBS deployment locations for passive micro-seismicity recording.

3.1 Ocean-bottom seismograph deployments

A total of 25 deployments were made throughout the cruise. Fig. 9 shows the actual deployment locations and instrument numbers, and exact deployment positions can be found in Table 2. OBS deployment was preceded by three acoustic release test dips conducted to 1000m. Two were conducted during the transit and one in the work area (see Table 3), together with a sound velocity profile to calibrate the swath bathymetry data.

3.2 Sound velocity profiling

A sound velocity profile was conducted in the north of the work area (see Table 3 for deployment location) using a Valeport Midas sound velocity probe. The resulting profile is shown in Fig. 10.

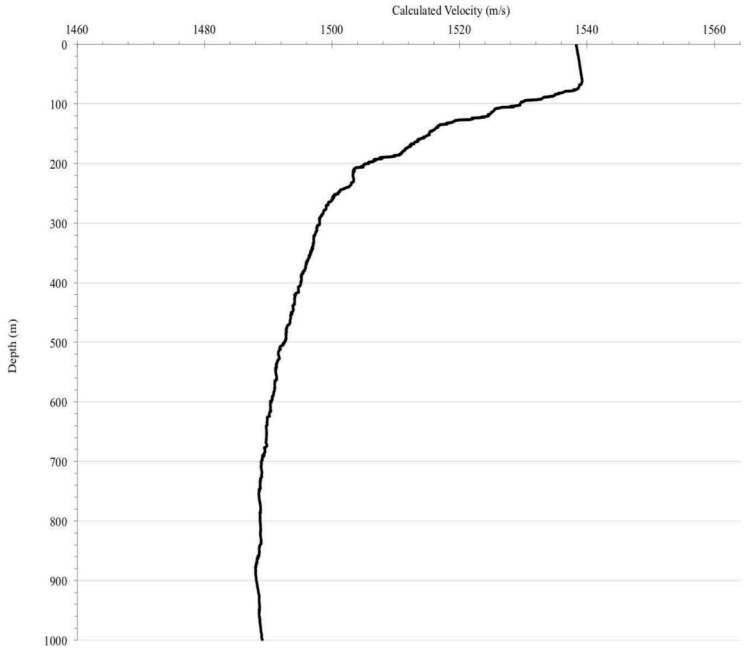

Figure 10: Sound velocity profile.

3.3 Gravity

Gravity data were acquired using a Lacoste-Romberg air-sea gravimeter (Model S-40) mounted on a gyro-stabilised platform. The gravimeter was "tied-in" to relative gravity base stations established on the quay prior to sailing. The original Port of Spain base station is located at the airport, and is now inaccessible. The relative gravity data will be tied to absolute gravity by two base ties against the absolute base station located at the NOC in Southampton when the vessel returns in June 2014 and prior to sailing for the recovery leg in October 2014. An example unprocessed data profile from the cruise is shown in Fig. 11. The gravity base station details are summarised in Table 4.

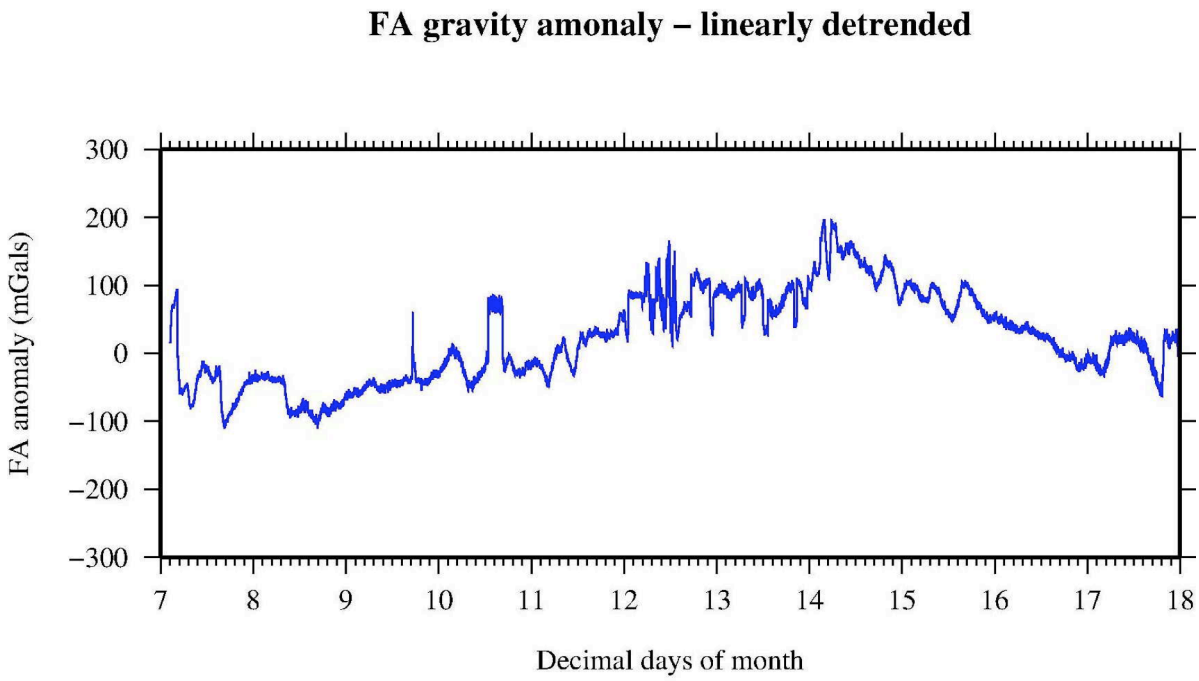

Figure 11: Example relative gravity data for cruise.

3.4 Swath bathymetry data

The RRS James Cook is fitted with a Kongsberg Simrad EM120 multi-beam deep ocean echo sounder. Data acquisition is based on successive transmit-receive cycles with the beam width optimised to match the sea conditions. Seabed depth and reflectivity are recorded against GMT time and GPS location. Swath bathymetry data were acquired port-to-port although, for the outbound leg with the sea and wind on the bow, data quality is relatively poor. Similarly, throughout the work area tracks run in the northerly direction were similarly affected. All other profile directions, including the return leg to port, provided data of good quality. A map showing all swath bathymetry data acquired is shown in Fig. 12, with that specific to the work area shown in Fig. 13.

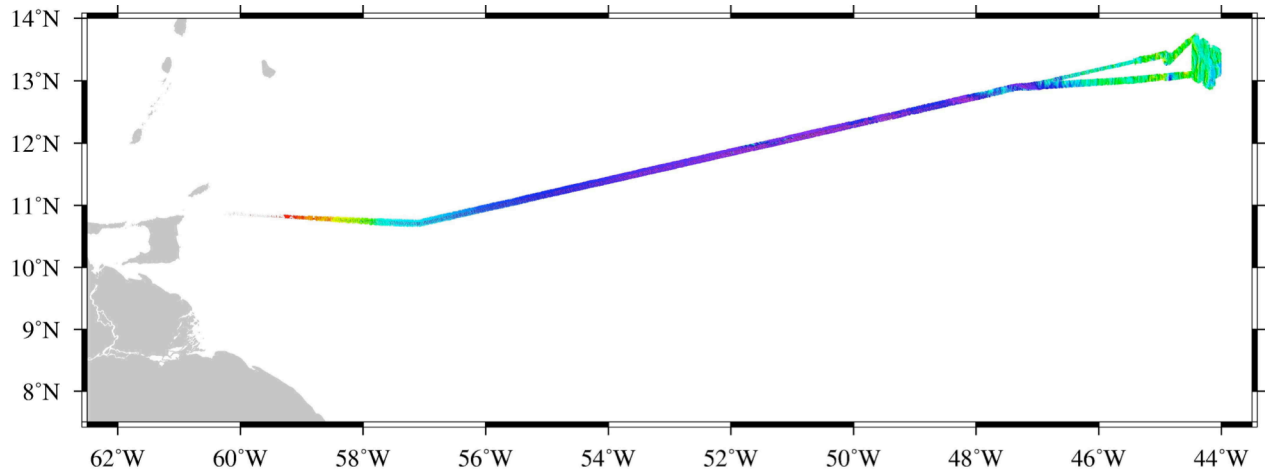

Figure 12: Swath bathymetry for entire cruise.

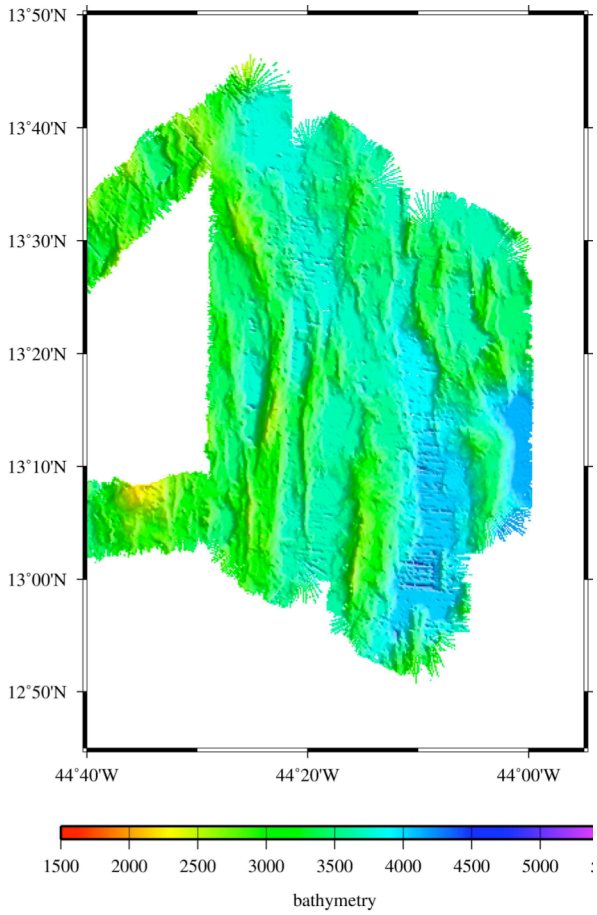

Figure 13: Swath bathymetry for work area.

4. Cruise narrative

The duration of the cruise was 11 days and 14 hours. Of this, ~9.5 days were spent on passage to and from Port of Spain to the work area, leaving a total of ~2 days in the work area. Of the latter ~0.5 days were spent deploying OBSs and ~1.5 days for swath bathymetry acquisition.

A summary of the events that took place appears below. All times are in GMT and all way points are listed in Table 1 and a cruise track charts are plotted in Figs 7 and 8.

Julian Day	Date	Time (GMT)	Activity
96	Sunday 6th April	22:30	Sailed from Port of Spain. GMT-4.
97	Monday 7th April	All day	On passage.
98	Tuesday 8th April	All day	On passage.
99	Wednesday 9th April	All day	On passage.
100	Thursday 10th April	00:00 13:00 16:25	On passage. Changed clocks GMT-3. Hove to. Acoustic release tests (WP ACOUSTIC). Acoustic tests complete. Recommence passage.
101	Friday 11th April	00:00	On passage.
102	Saturday 12th April	01:00 04:30 05:10 05:38 06:01 06:25 06:50 07:17 07:47 08:06 08:34 08:54 09:12 09:37 10:00 10:25 10:52 11:06 11:27 11:34 11:47 12:11 12:25 12:40 12:54 13:08 13:23 13:25 17:20	Hove to in work area. Acoustic release tests. Acoustic tests complete. Transit to OBS 1. OBS 1 deployed (WP OBS_1). OBS 2 deployed (WP OBS_2). OBS 3 deployed (WP OBS_3). OBS 4 deployed (WP OBS_4). OBS 5 deployed (WP OBS_5). OBS 6 deployed (WP OBS_6). OBS 7 deployed (WP OBS_7). OBS 8 deployed (WP OBS_8). OBS 9 deployed (WP OBS_9). OBS 10 deployed (WP OBS_10). OBS 11 deployed (WP OBS_11). OBS 12 deployed (WP OBS_12). OBS 13 deployed (WP OBS_13). OBS 14 deployed (WP OBS_14). OBS 15 deployed (WP OBS_15). OBS 16 deployed (WP OBS_16). OBS 17 deployed (WP OBS_17). OBS 18 deployed (WP OBS_18). OBS 19 deployed (WP OBS_19). OBS 20 deployed (WP OBS_20). OBS 21 deployed (WP OBS_21). OBS 22 deployed (WP OBS_22). OBS 23 deployed (WP OBS_23). OBS 24 deployed (WP OBS_24). OBS 25 deployed (WP OBS_25). Transit to swath survey waypoint SW_1. Commencing swath survey at point A (WP

			SW_1). 22:08 Arrival at swath survey point B (WP SW_2). 23:05 Arrival at swath survey point C (WP SW_3).
103	Sunday 13th April	06:21 07:13 11:53 13:13 19:52 20:45 20:45	Arrival at swath survey point D (WP SW_4). Arrival at swath survey point E (WP SW_5). Arrival at swath survey point F (WP SW_6). Arrival at swath survey point G (WP SW_7). Arrival at swath survey point H (WP SW_8). Arrival at swath survey point I (WP SW_9). Change course 270º to conduct swath calibration across all lines.
104	Monday 14th April	02:40	Swath survey complete. Start passage to Port of Spain.
105	Tuesday 15th April	All day	On passage.
106	Wednesday 16th April	All day	On passage.
107	Thursday 17th April	00:00 All day	Changed clocks GMT-4. On passage.
108	Friday 18th April	13:00 15:00	Arrived Port of Spain anchorage. Hove to. Boat transfer of personnel.
109	Saturday 19th April	16:30 23:55	Boat transfer of personnel. Alongside.

5. Equipment performance

5.1 Ocean-bottom seismographs

The OBS will be recovered during JC109 and a commentary of their performance will be found in the report for that cruise.

5.2 All other equipment

All other ship based equipment functioned perfectly throughout use.

5.3 Ship's machinery and fitted equipment

Apart from the Bridge communications unit that failed just prior to departure, all other ship's fitted equipment and machinery functioned without problem throughout the cruise.

6. Demobilisation

This only being an instrument deployment cruise, the remaining OBS supplementary equipment was packed into its 20' shipping container during the transit back to port and sealed prior to arrival. On arrival at the berth the container was off-loaded and consigned to the care of the agent for delivery to the shipping line for return to the UK.

Acknowledgements

We would like to thank the master, officers and crew of the *RRS James Cook* and the support staff and sea-going technicians of NERC's National Marine Facility (NMF) for their efforts and good humour throughout this cruise. We would particularly like to thank Jez Evans, the Cruise Project Manager, whose organisation and management throughout was greatly appreciated by the scientific party. Finally, we particularly thank Ben Pitcairn and Andrew Clegg from the NERC's Ocean-Bottom Instrumentation Facility (OBIF) for their efficient and professional ocean-bottom instrument support. This research was funded by the U.K.'s Natural Environment Research Council under their standard grants scheme.

References

Baines, G.B., et al., 2008. *EPSL*, **273,** 105-114**.**
Buck, W.R., et al., 2005. *Nature,* **434**, 719-723
Canales, J.P., et al., 2008. *G*^{3}*,* **9**, Q08002
Cann, J.R. et al., 1997. *Nature,* **385**, 329-332
Cannat, M., et al., 2010. *AGU Geophys. Mono. Series,* **188**, 241-264.
Connelly, D., et al., 2011. *Nature Comms*., **3**, 620.
deMartin, B, et al., 2007. *Geology*, **35**, 711-714.
Dick, H.J.B., et al., 2008. *G*^{3}, **9**, Q05014.
Escartin, J. et al., 2008. *Nature,* **455**, 790-795.
Escartin, J & Canales, J-P, 2011, *EOS Trans. AGU* ***92***(4), 31-32.
Grimes, C.B., et al. 2008. *G*^{3}, **9**, Q08012.
Ildefonse, B., et al., 2007. *Geology,* **35**, 623–626.
Lavier, L.L., et al., 1999. *Geology*, **27**, 1127-1130.
MacLeod, C.J., et al., 2002. *Geology,* **30**, 879-882.
MacLeod, C.J., et al., 2009. *EPSL,* **287**, 333-344.
MacLeod, C.J., et al., 2011. *G*^{3}, 12, Q0AG03.
Mallows C. & Searle R., 2012, *G*^{3}, **13**, Q0AG08.
Mallows, C. 2011. Unpubl PhD thesis, U. Durham
Morris, A., et al., 2009. *EPSL*, **287**, 217–228.
Okino, K., et al., 2004. *G*^{3}, 5, Q12012.
Olive, J.A., et al., 2010. *Nature Geoscience***, 3,** 491-195.
Peirce, C. & Day, A.J., 2002. *Geophys. J. Int*., **151**, 2, 543-566.
Reston, T.J. & Ranero, C.R. 2011 *G*^{3}, **12**, Q0AG05..
Reston TJ et al., 1999. *JGR*, **104**, 629-644.
Schouten, H., et al., 2010. *Geology,* **38**, 615-618.
Searle, R. C. et al., 2003. *G*^{3}, **4**, 9105, doi:10.1029/2003GC000519.
Searle, R.C., et al., 2007. RRS James Cook Cruise JC007: Cruise Report, Durham University, 59pp.
Smith, D.K., et al., 2008. *G*^{3}*,* **9**, Q03003
Tucholke, B.E. & Lin, J., 1994. *JGR*, **99**, 11,937-11,958.
Tucholke, B.E., et al., 1998. *JGR,* **103**, 9857- 9866.
Tucholke, B.E., et al., 2008. *Geology,* **36**, 455-458

Tables

Table 1 - Way points

WAYPOINTS

NAME		(N)	(W)		Lat Deg	North Min	Long Deg	West Min	Long Deg	East Min	Long (E)
TRANSIT	Boundary between Trinidad & Tobago and Barbados waters	10.7000	57.0833	approx	10	42.00	57	5.00	302	55.00	302.9167
ACOUSTIC	acoustics tests	13.4300	44.8800		13	25.80	44	52.80	315	7.20	315.1200

OBS LOCATIONS		**PASSIVE OBS ARRAY**									
	OBS No.	(N)	(W)	Depth (m)	Lat Deg	North Min	Long Deg	West Min	Long Deg	East Min	Long (E)
OBS_1	1	13.4065	44.8765	3881	13	24.390	44	52.590	315	7.410	315.1235
OBS_2	2	13.4075	44.8900	3887	13	24.450	44	53.400	315	6.600	315.1100
OBS_3	3	13.4075	44.9120	3323	13	24.450	44	54.720	315	5.280	315.0880
OBS_4	4	13.3915	44.9260	3167	13	23.490	44	55.560	315	4.440	315.0740
OBS_5	5	13.3915	44.9050	3503	13	23.490	44	54.300	315	5.700	315.0950
OBS_6	6	13.3910	44.8850	3946	13	23.460	44	53.100	315	6.900	315.1150
OBS_7	7	13.3905	44.8660	3510	13	23.430	44	51.960	315	8.040	315.1340
OBS_8	8	13.3750	44.8565	3495	13	22.500	44	51.390	315	8.610	315.1435
OBS_9	9	13.3765	44.8790	3647	13	22.590	44	52.740	315	7.260	315.1210
OBS_10	10	13.3765	44.8990	3585	13	22.590	44	53.940	315	6.060	315.1010
OBS_11	11	13.3780	44.9155	3484	13	22.680	44	54.930	315	5.070	315.0845
OBS_12	12	13.3660	44.9065	3321	13	21.960	44	54.390	315	5.610	315.0935
OBS_13	13	13.3620	44.8915	3690	13	21.720	44	53.490	315	6.510	315.1085
OBS_14	14	13.3635	44.8700	3382	13	21.810	44	52.200	315	7.800	315.1300
OBS_15	15	13.3570	44.8480	3372	13	21.420	44	50.880	315	9.120	315.1520

OBS_16	16	13.3430	44.8600	3485	13	20.580	44	51.600	315	8.400	315.1400
OBS_17	17	13.3485	44.8790	3484	13	20.910	44	52.740	315	7.260	315.1210
OBS_18	18	13.3490	44.8995	3464	13	20.940	44	53.970	315	6.030	315.1005
OBS_19	19	13.3550	44.9190	2973	13	21.300	44	55.140	315	4.860	315.0810
OBS_20	20	13.3350	44.8885	3248	13	20.100	44	53.310	315	6.690	315.1115
OBS_21	21	13.3290	44.8690	3478	13	19.740	44	52.140	315	7.860	315.1310
OBS_22	22	13.3300	44.8495	3379	13	19.800	44	50.970	315	9.030	315.1505
OBS_23	23	13.3130	44.8615	3267	13	18.780	44	51.690	315	8.310	315.1385
OBS_24	24	13.3160	44.8835	3328	13	18.960	44	53.010	315	6.990	315.1165
OBS_25	25	13.3010	44.8770	3540	13	18.060	44	52.620	315	7.380	315.1230
	SWATH										
SW_1	A	13.7220	44.4260		13	43.320	44	25.560	315	34.440	315.5740
SW_2	B	13.0655	44.4274		13	3.930	44	25.644	315	34.356	315.5726
SW_3	C	13.0203	44.3352		13	1.218	44	20.112	315	39.888	315.6648
SW_4	D	13.6408	44.3337		13	38.448	44	20.022	315	39.978	315.6663
SW_5	E	13.5776	44.2413		13	34.656	44	14.478	315	45.522	315.7587
SW_6	F	12.9661	44.2430		12	57.966	44	14.580	315	45.420	315.7570
SW_7	G	12.9209	44.1509		12	55.254	44	9.054	315	50.946	315.8491
SW_8	H	13.5234	44.1489		13	31.404	44	8.934	315	51.066	315.8511
SW_9	I	13.4692	44.0566		13	28.152	44	3.396	315	56.604	315.9434
SW_10	J	12.8666	44.0588		12	51.996	44	3.528	315	56.472	315.9412
SW_11	K	12.8213	43.9667		12	49.278	43	58.002	316	1.998	316.0333
SW_12	L	13.6307	43.9635		13	37.842	43	57.810	316	2.190	316.0365
SW_13	M	13.9108	44.4256		13	54.648	44	25.536	315	34.464	315.5744
SW_14	N	14.0457	44.4254		14	2.742	44	25.524	315	34.476	315.5746
SW_15	O	14.0456	44.3605		14	2.736	44	21.630	315	38.370	315.6395
SW_16	P	13.9556	44.3329		13	57.336	44	19.974	315	40.026	315.6671
SW_17	Q	13.7296	43.9631		13	43.776	43	57.786	316	2.214	316.0369
SW_18	R	13.8376	43.9627		13	50.256	43	57.762	316	2.238	316.0373
SW_19	S	14.0454	44.2956		14	2.724	44	17.736	315	42.264	315.7044
SW_20	T	14.0633	44.2492		14	3.798	44	14.952	315	45.048	315.7508
SW_21	U	14.1082	44.2212		14	6.492	44	13.272	315	46.728	315.7788
SW_22	V	13.9455	43.9623		13	56.730	43	57.738	316	2.262	316.0377
SW_23	W	14.0534	43.9618		14	3.204	43	57.708	316	2.292	316.0382
SW_24	X	14.1800	44.1654		14	10.800	44	9.924	315	50.076	315.8346

Table 2 - OBS deployment locations

OBS No.	(N)	(W)	Depth (m)	Deg	Min	Deg	Min	Deg	Min	(E)
1	13.4065	44.8766	3649	13	24.393	44	52.597	315	7.403	315.1234
2	13.4075	44.8899	3643	13	24.447	44	53.396	315	6.604	315.1101
3	13.4074	44.9119	3274	13	24.446	44	54.717	315	5.283	315.0881
4	13.3917	44.9260	3047	13	23.503	44	55.558	315	4.442	315.0740
5	13.3915	44.9052	3449	13	23.493	44	54.312	315	5.688	315.0948
6	13.3910	44.8850	3790	13	23.461	44	53.102	315	6.898	315.1150
7	13.3906	44.8661	3464	13	23.435	44	51.963	315	8.037	315.1339
8	13.3751	44.8565	3473	13	22.508	44	51.387	315	8.613	315.1435
9	13.3765	44.8791	3544	13	22.587	44	52.746	315	7.254	315.1209
10	13.3765	44.8989	3474	13	22.588	44	53.936	315	6.064	315.1011
11	13.3780	44.9155	3424	13	22.678	44	54.927	315	5.073	315.0845
12	13.3660	44.9065	3111	13	21.962	44	54.387	315	5.613	315.0936
13	13.3620	44.8916	3606	13	21.721	44	53.495	315	6.505	315.1084
14	13.3635	44.8700	3424	13	21.811	44	52.200	315	7.800	315.1300
15	13.3570	44.8480	3212	13	21.423	44	50.881	315	9.119	315.1520
16	13.3429	44.8601	3481	13	20.573	44	51.604	315	8.396	315.1399
17	13.3483	44.8791	3498	13	20.899	44	52.749	315	7.251	315.1209
18	13.3488	44.8997	3437	13	20.931	44	53.982	315	6.018	315.1003
19	13.3548	44.9192	2981	13	21.289	44	55.151	315	4.849	315.0808
20	13.3349	44.8885	3203	13	20.091	44	53.311	315	6.689	315.1115
21	13.3290	44.8692	3458	13	19.738	44	52.152	315	7.848	315.1308
22	13.3300	44.8494	3329	13	19.802	44	50.963	315	9.037	315.1506
23	13.3128	44.8617	3258	13	18.765	44	51.703	315	8.297	315.1383
24	13.3156	44.8837	3176	13	18.934	44	53.021	315	6.979	315.1163
25	13.3010	44.8772	3486	13	18.062	44	52.631	315	7.369	315.1228

Table 3 - Sound velocity profile and acoustic tests

	Day	Time GMT	Latitude (N)		Longitude (W)	
			Deg	Min	Deg	Min
Acoustic test 1 &2	100	13:00	12	17.5596	49	58.7501
Acoustic test 3 & SVP	102	01:00	13	25.7282	44	52.9582

Table 4 - Gravity base stations

	Latitude (N)		Longitude (W)	
	Deg	Min	Deg	Min
SE corner customs warehouse	10	39.1217	61	31.1817
Quayside RRS Cook – pre-cruise Between bollard 32 and 33 0.77m north of the second crack in the concrete south from bollard 33	10	39.1367	61	31.2150
Quayside RRS Cook – post-cruise Between bollard 37 and 38 2.7m north of the second crack in the concrete north from bollard 37	10	39.1667	61	31.2667

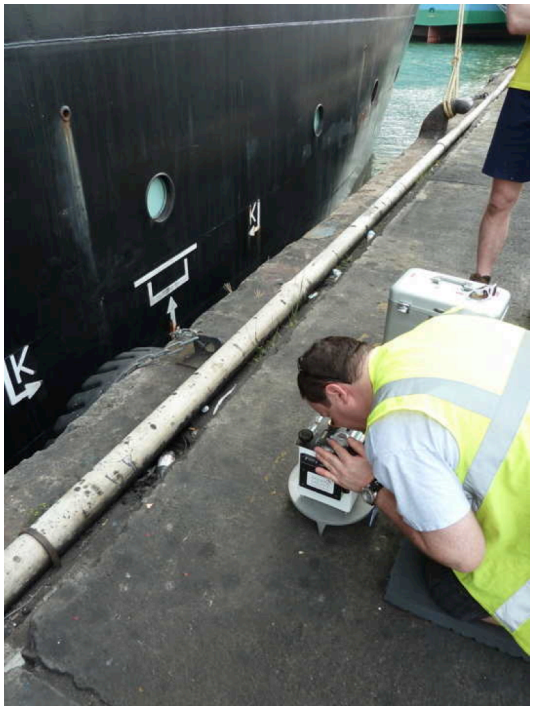

Quayside gravity base station location – second crack in foreground, bollard 33 in background

Table 5 - Scientific personnel

The RRS Discovery carried a total crew of 28 people for cruise JC102 as named below:

Master	John Leask
Chief Officer	Peter Newton
2nd Officer	Iain Macleod
3rd Officer	Nick Norrish
Chief Engineer	Robert Lucas
2nd Engineer	Christopher Kemp
3rd Engineer	Gary Slater
3rd Engineer	Frank Dowitt
ETO	Paul Damerell
ERPO	John Smyth
CPO(Science)	John MacDonald
CPO (Deck)	Andrew MacLean
PO (Deck)	John Hopley
Seaman	David Dalzell
Seaman	Mark Ord
Seaman	Graham Bartlett
Seaman	Steven Day
Purser	Graham Bullimore
Head Chef	John Haughton
Chef	Walter Link
Steward	Graham Mingay
Assistant Steward	Kevin Mason
Principal Scientist	Christine Peirce
Scientist	Matthew Funnell
OBS Support	Ben Pitcairn
OBS Support	Andrew Clegg
Techical Liaison Officer	Mark Maltby
Technical Support	Andrew Moore

Table 6 - Project 13N Principal Scientists, Project Partners and Consultants

The Principal Scientists, Project Partners and Consultants for the *13N MAR* project are:

Principal Scientists:	Professor Tim Reston (Birmingham University) Professor Christine Peirce (Durham University) Professor Chris MacLoed (Cardiff University)
Project Partners:	Dr Robert Sohn (Woods Hole Oceanographic Institution) Dr Juan Pablo Canales (Woods Hole Oceanographic Institution) Dr Javier Escartin (Institute de Physique de Globe, Paris)
Consultants:	Professor Roger Searle (Emeritus, Durham University) Professor Joe Cann (Emeritus, Leeds University)